A New Operational Solar Resource Forecast Model Service for PV Fleet Simulation

Richard Perez[1], Adam Kankiewicz[2], James Schlemmer[1], Karl Hemker, Jr.1 and Sergey Kivalov[1]

[1] Atmospheric Sciences Research Center, the University at Albany, Albany, New York, 12203, USA
[2] Clean Power Research, Napa, California, 94558, USA

***Abstract* — We present and evaluate a new operational solar radiation forecast model to be deployed on a prototype basis as part of the SolarAnywhere (SA) data service. The SA service covers North America and provides seamless access to historical, real time and forecasted solar irradiance data with a maximum possible geographical resolution of 1 km and a maximum time resolution of 1 minute for historical and real time data. The new forecast product presented in this article pertains to SA's intermediate spatial and temporal resolution data, respectively 10 km and hourly. The forecast time horizon ranges from one hour ahead to five days ahead.**

***Index Terms* — solar resource, forecast, simulation, irradiance.**

I. Introduction

Solar resource forecasts are essential to facilitating the integration of variable energy resources such as PV electricity onto the electrical grid. Short-term (1-5 hours) forecasts are important for optimizing the deployment of stand-by storage and/or variable generation technologies: a recent study by Perez et al. [1] showed that accurate forecasts can reduce the cost of short term variability mitigation by nearly 50%. Next-day and multi-day forecasts are important to optimally participate in energy markets as well as to optimize the operation of variable generation assets with longer lead times.

II. Methods

The new forecast model consists of an optimum mix of satellite-derived cloud motion forecasts [2,3], the National Digital Forecast Database's (NDFD) cloud cover-derived irradiance forecasts, and several operational numerical weather prediction (NWP) models including the following global and continental-scale models: The National Center for Environmental Prediction's (NCEP) Global Forecast System (GFS) forecasts [4], the European Centre for Medium-Range Forecasts (ECMWF) [5], NCEP's North American Mesoscale (NAM) forecasts [6], and NCEP's rapid update assimilation models including the Rapid Refresh (RAP) and High Resolution Rapid Refresh (HRRR) forecasts [7, 8]. The satellite-to-irradiance model underlying the cloud motion forecasts is a new version of the SA model that utilizes the satellite's infrared channels in addition to its visible channel [9]. Therefore the cloud motion model is capable of detecting pre-dawn clouds and cloud motion; hence it is capable of producing cloud motion forecasts effective from sunrise onward, unlike SA's previous cloud motion model [2] that could only initiate forecasts after sunrise.

The underlying models' spatial and temporal granularity, refresh frequency, and time horizons are presented in Table 1.

TABLE I
UNDERLYING MODELS SPATIAL AND TEMPORAL RESOLUTION

Model	Spatial Resolution	Coverage	Refresh Rate	Time Resolution	Time Horizon
National Digital Forecastt Database (NDFD)	5 km	USA	3-hourly	3 hours	168 hours
Rapid Update (RAP)	13 km	North America	hourly	1 hour	18 hours
North American Mesoscale (NAM)	12 km	North America	6-hourly	1 / 3 hours *	84 hours
Global Forecast System (GFS)	~50 km	Global	6-hourly	3 / 12 hours **	384 hours
European Ctr for Medium Range Weather Forecasts (ECMWF)	~13 kn	Global	12-hourly	3 / 6 hours ***	240 hours
High Resolution Rapid Refresh (HRRR)	3 km	North America	hourly	1 hour	18 hours
Satellite cloud motion	10 km	Global****	hourly	1 hour	9 hours

** 1 hour until 36 hours ahead, 3 hours beyond ** 3 hours until 192 hours ahead, 12 hours beyond *** 6 hours until 144 hours ahead, 6 hours beyond ****currently operational in North America*

The performance of the new model and that of its underlying NWP and cloud motion models is benchmarked against ***smart persistence*** forecasts for the four test locations listed in Table 2. Persistence consists of projecting current irradiance conditions into the future by assuming a constant clear sky index, but accounting for fully predictable solar geometry changes. Smart persistence consists of lengthening the time interval defining current conditions as a function of the considered forecast time horizon [10].

A configuration of the new model including smart persistence in the mix of models is also evaluated – this configuration would be applied when irradiance measurements are available, as would be the case for large power plants.

The performance of the new model is also gauged against the performance of the previous version of the SA forecast model that had been operational since its inception in 2009 [11]. This previous model consisted of a simple combination of satellite derived cloud motion irradiance forecasts and NDFD forecasts.

TABLE II
GROUND TRUTH LOCATIONS

Location	latitude	Longitude	Elevation	Prevailing Climate	Data Source
Hanford, CA	36.31° N	119.63° W	73 m	Semi-arid	NOAA-ISIS
Desert Rock, NV	36.63° N	116.02° W	1007 m	Arid	NOAA- SURFRAD
Goodwin Creek, MS	34.25° N	89.87° W	98 m	Warm continental	NOAA- SURFRAD
Penn State, PA	40.72° N	77.93° W	376 m	Cold continental	NOAA- SURFRAD

III. RESULTS

Figure 1 illustrates the comparative performance of all the considered models as quantified by their relative RMSE plotted against forecast time horizon up to 130 hours ahead. These results are based on the analysis of 10 months of hourly data spanning June 2013 through April 2014. Also plotted in Figure 1 for reference purposes is the performance of the [non-forecast] intermediate resolution satellite-to-irradiance conversion model. The top graph shows model performance for the four locations combined, while the four bottom graphs illustrate model performance at individual locations.

Because the objective of the SA forecast service is to deliver predicted hourly irradiances with an hourly refresh rate, all models are treated as hourly production models and compared against all the measured hourly data points. For the models with a time resolution or a refresh rate exceeding one hour, this implies interpolation or extrapolation of predicted values, as well as having to [conservatively] accept forecasts with longer lead times for a given forecast time horizon. This is, of course, fully reflected in the performance of the new SA model that is built, in part, from such lower time resolution/refresh rate models.

Results are consistent with past observations by the authors and others (e.g., see [12]) showing the ECMWF global model as best performing of the forecast models for all but very short term time horizons, where the cloud motion model performs best. The performance of the high-resolution assimilation models -- RAP and HRRR -- is disappointing with RMSEs much in excess of persistence and the other considered NWP models to the exception of the NAM. A possible reason is that their high resolution introduces localized cloud variability which cannot exactly resolve observed cloud fields. A similar reason was advanced for explaining the modest performance of the high resolution WRF model when compared to lower resolution global models [12].

The new optimal combination model (labelled as Model-1 in Figure 1) performs considerably better than all its underlying models and remains on par or better than the reference satellite model up to two hours ahead. In Penn State and Desert Rock, the performance of the new forecast model remains comparable to the satellite reference up to several hours ahead (up to 24 hours ahead for Desert Rock). Including smart persistence as an input to the new model (Model-2) results in a substantial performance improvement for the one-hour ahead forecast, a marginal improvement for the two-hour forecast horizon, and no improvement beyond. Also reported in the individual site graphs is the performance of a model resulting from a mix of models which was not optimized for these individual sites, but from the ensemble of the test locations. The RMSE of this site-independent model is represented by the thick orange lines in each of the bottom graphs. Minor performance degradation is observed, however it remains considerably better than the underlying models.

An interesting feature of the smart persistence is that it tends to perform better at the 24 hour horizon than at the 6-to-12 hours horizons, particularly at predominantly clear sites with a propensity for diurnal cloud formation (Desert Rock and Hanford). This effect is not apparent at Penn State and Goodwin Creek where clouds tend to result from frontal passages. Also note how smart persistence's RMSE remains ~ level beyond 24 hours. This is unlike conventional persistence

previously used by the author and colleagues [12] which continues to increase monotonously beyond one day ahead.

As such smart persistence is a considerably more stringent benchmark of model performance than the previously used persistence. Forecasting ***skill*** is used here in reference to this more stringent benchmark, and defined as one minus the ratio between smart persistence RMSE and the considered model RMSE. With this definition, a skill of zero represents no improvement over the reference benchmark and a skill of one represents a perfect forecast.

Figure 2 compares the forecasting skills of the existing SolarAnywhere model and the new model – note that the existing SA model is highlighted by the thick, semi-transparent lines in Figure 1, switching from cloud motion for short term forecasts to NDFD for longer time horizons.

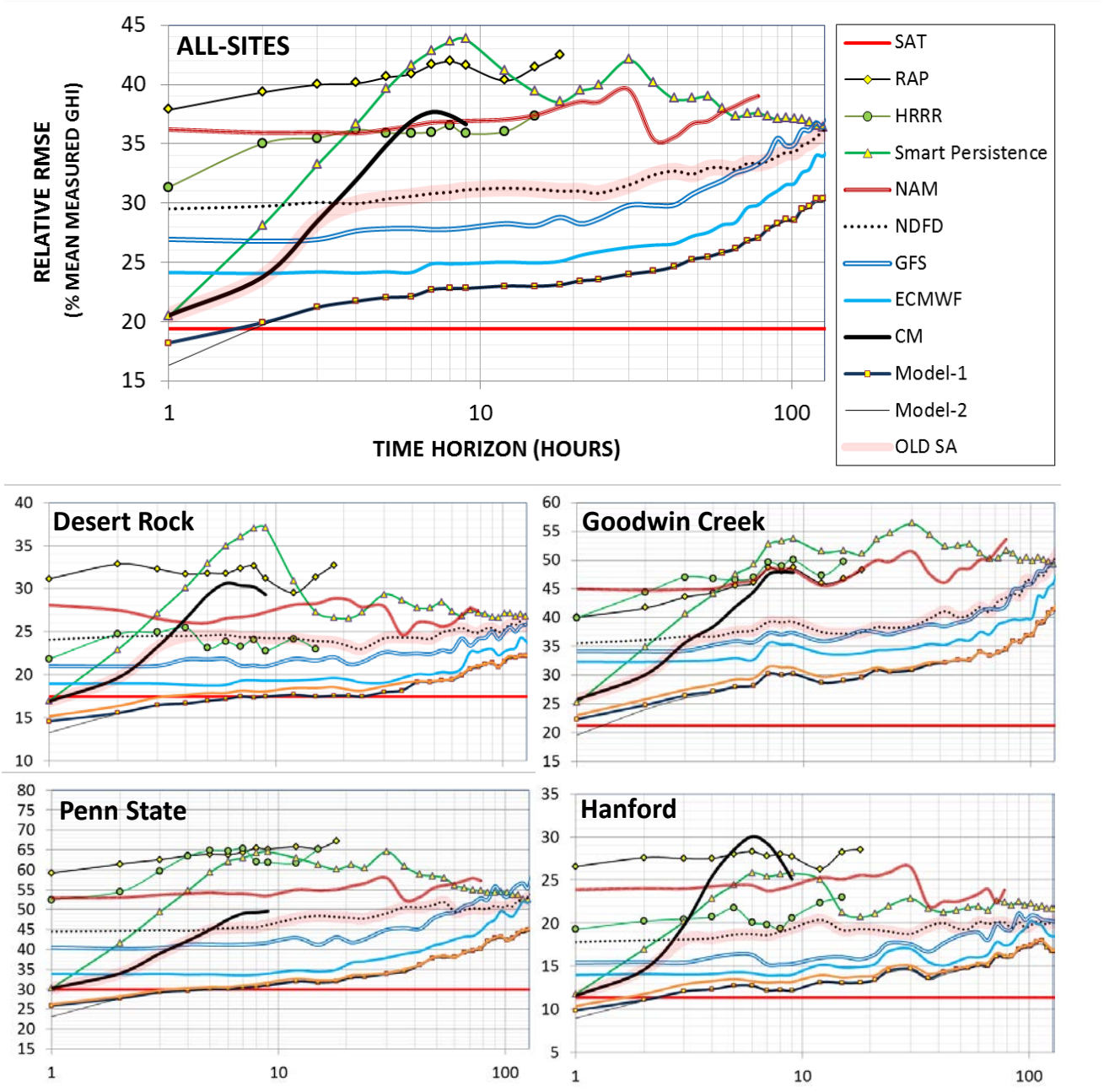

Fig. 1. Comparing Model RMSEs as a function of forecast time horizon. The additional orange line in the individual site graphs represents a model mix that is not site-optimized but common to all sites.

The forecasting skills of the new and existing SolarAnywhere model are presented as a function of time horizon for the 4-sites combination (top graph) and for each individual site (bottom graphs). Skill peaks at ~50% for 10-hour forecasts and remains near 40% for up to 30-hour forecasts. At 130 hours (five days ahead), the skill of the new SA model remains nearly at 20% while it falls down to zero for the old SA model. Skill improvement from the old to the new SA forecast model is shown in Figure 3. Improvement is near or greater than 100% for all sites and tends to increase with time horizon except for Hanford, where RMSEs are generally small and the weather is very stable.

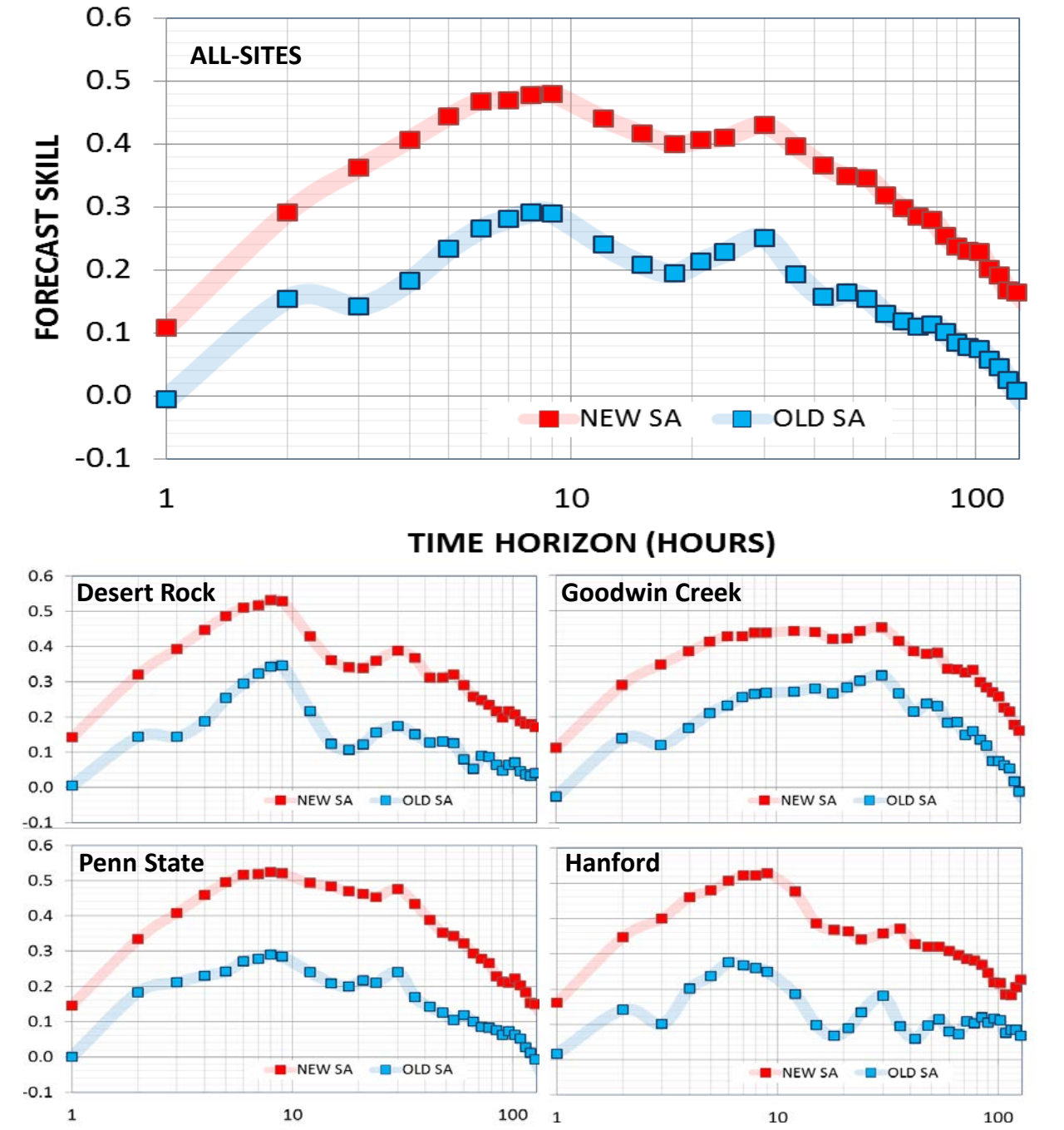

Fig. 2. Comparing skills of the current and new SA forecasts.

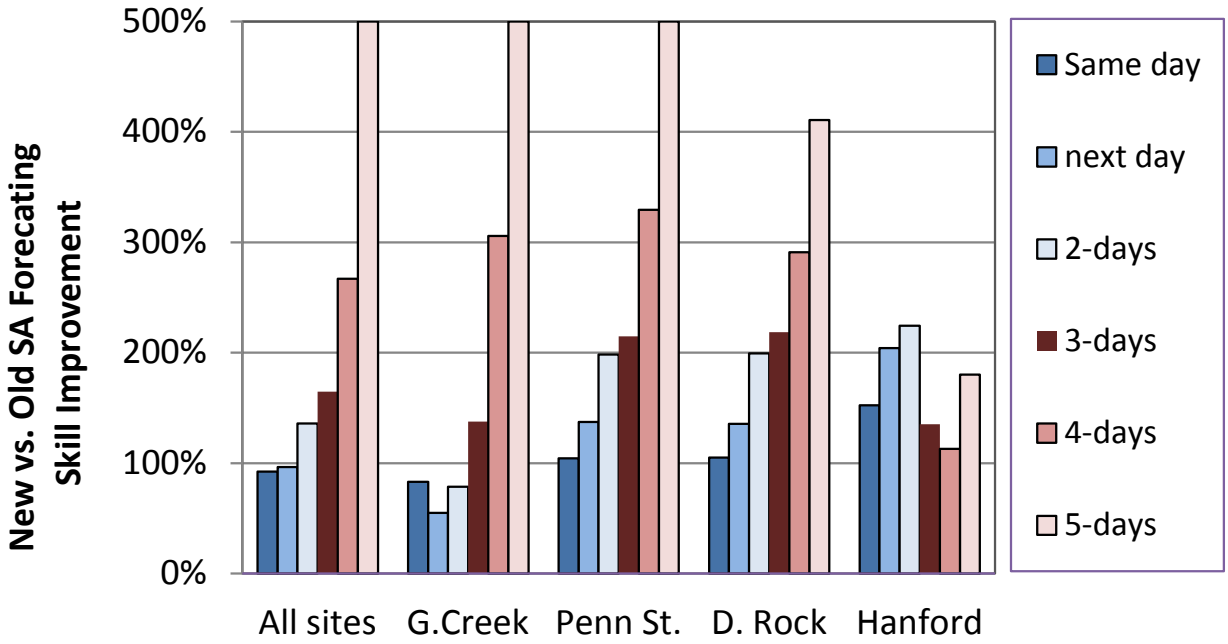

Fig. 3. Forecast skill improvement

Figure 4 provides a qualitative appreciation of model performance by comparing forecast-vs-measured irradiance scatterplots for the smart persistence, the old SA, the new SA and the ECMWF model at the one hour and 24-hours time horizons.

IV. Concluding Remarks

We have presented a new operational irradiance forecast model consisting of an optimum mix of existing operational models. This new model, to be deployed on a prototype basis as part of the SolarAnywhere service, performs better than its underlying components and results in a substantial gain in performance over the current version of the operational SolarAnywhere model.

The present exercise focused on global irradiance (GHI) prediction. Future developmental and validation steps will focus on direct normal irradiance (DNI) where the effects of underlying model output combination and resulting dynamic range reduction are exacerbated by the non-linear GHI-DNI relationship. We also plan to investigate whether any of the underlying models could be corrected to remove possible systematic bias patterns as had previously been successfully undertaken for the NDFD model underlying the old SA forecast model [13].

References

[1] R. Perez, T. Hoff, J. Dise, D. Chalmers and S. Kivalov (2013), "Mitigating Short-Term PV Output Variability," *Proceedings of 28th European Photovoltaic Solar Energy Conference and Exhibition (EUPVSEC), Paris, France*, 2013.

[2] R. Perez, S. Kivalov, J. Schlemmer, K. Hemker Jr., D. Renné, and T. Hoff, "Validation of Short and Medium Term Operational Solar Radiation Forecasts in the US," *Solar Energy*, vol. 84, 12, pp. 2161-2172, 2010.

[3] E. Lorenz, J. Hurka, D. Heinemann, H.G. Beyer, "Irradiance Forecasting for the Power Prediction of Grid-Connected Photovoltaic Systems," *IEEE Journal of Special Topics in Earth Observations and Remote Sensing*, vol. 2, pp. 2–10, 2009.

[4] GFS, "Global Forecasting System," http://www.emc.ncep.noaa.gov/index.php?branch=GFS, 2013.

[5] ECMWF, "European Centre for Medium-Range Weather Forecasts," http://www.ecmwf.int/, 2013.

[6] NAM, "North American Mesoscale Forecast System," http://www.ncdc.noaa.gov/data-access/model-data/model-datasets/north-american-mesoscale-forecast-system-nam, 2013.

[7] RAP, "Rapid Refresh," http://rapidrefresh.noaa.gov/ , 2013.

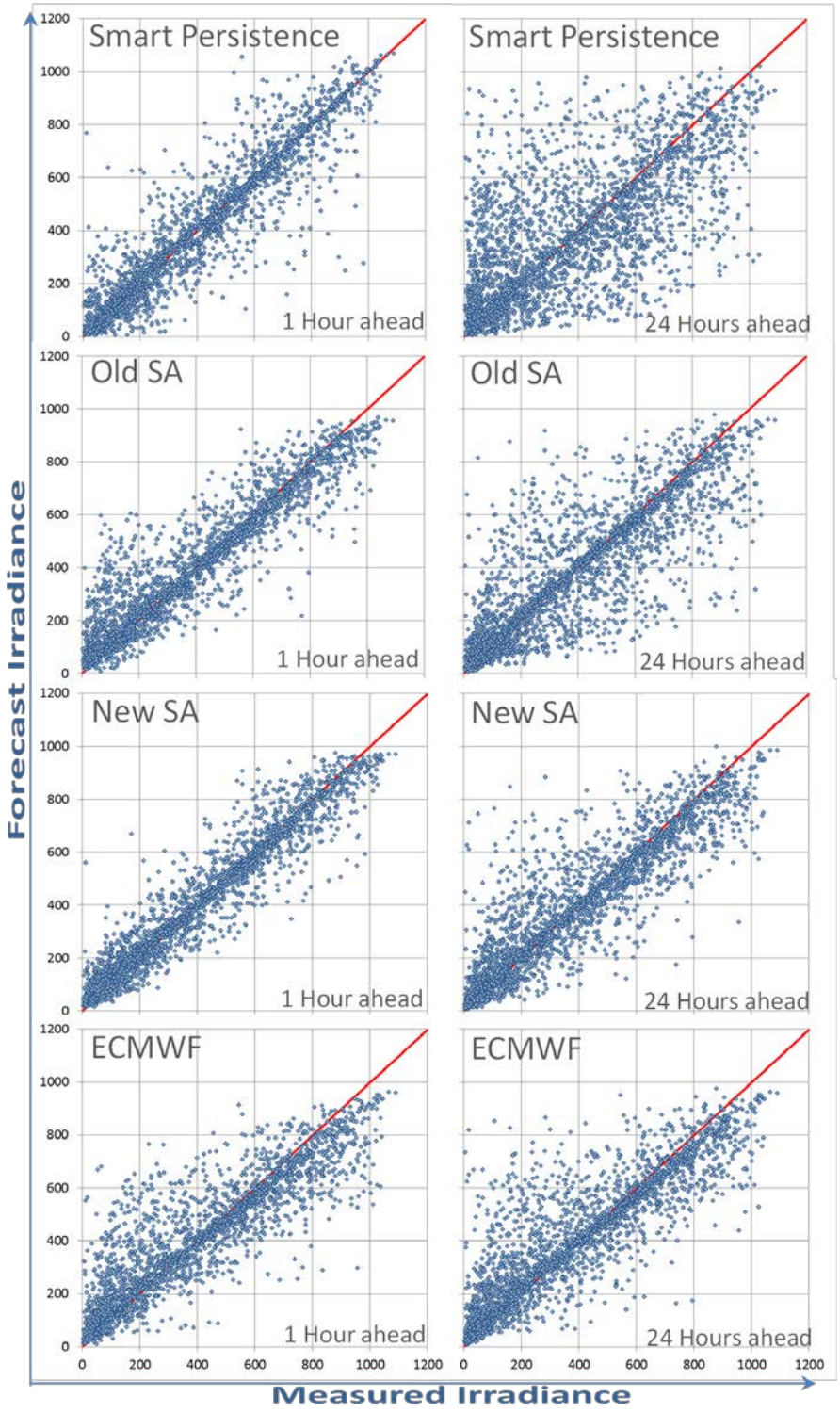

Fig. 4. One-hour and 24-hours ahead forecast vs. measured GHI irradiance in Goodwin Creek.

[8] HRRR, "The High-Resolution Rapid Refresh," http://ruc.noaa.gov/hrrr/, 2013.

[9] J. Dise, A. Kankiewicz, J. Schlemmer, K. Hemker, Jr., S. Kivalov, T. Hoff, & R. Perez, "Operational Improvements in the Performance of the SUNY Satellite-to-Solar Irradiance Model Using Satellite Infrared Channels," in *39th IEEE PV Specialists Conference*, 2013.

[10] IEA SHCP Task 36, "International Energy Agency, Solar Heating and Cooling Programme, Task 36 Solar Resource Knowledge Management, subtask A, model benchmarking," http://www.iea-shc.org/task36/, 2011.

[11] R. Perez and T. Hoff, SolarAnywhere Forecasting, in *Solar Resource Assessment and Forecasting*, Elsevier, 2013.

[12] R. Perez, E. Lorenz, S. Pelland, M. Beauharnois, G. Knowe, K. Hemker, Jr., D. Heinemann, J. Remund, S.C. Müller, W. Traunmüller, G. Steinmaurer, D. Pozo, J. A. Ruiz-Arias, V. Lara-Fanego, L. Ramirez, M. Gaston-Romeo, L. M. Pomares, "Comparison of numerical weather prediction solar irradiance forecasts in the US, Canada and Europe," *Solar Energy* vol. 94, pp. 305-320, 2013.

[13] R. Perez, K. Moore, S. Wilcox, D. Renné, and A. Zelenka, "Forecasting Solar Radiation – Preliminary Evaluation of an Approach Based upon the national Forecast Data Base," *Solar Energy*, vol. 81, 6, pp. 809-812, 2007.